Investigations on the structural, optical and electrical properties of Nb-doped SnO$_2$ thin films

V. Gokulakrishnan · S. Parthiban · K. Jeganathan · K. Ramamurthi

Abstract Niobium-doped tin oxide thin films were deposited on glass substrates by the chemical spray pyrolysis method at a substrate temperature of 400 °C. Effects of Nb doping on the structural, electrical and optical properties have been investigated as a function of niobium concentration (0–2 at.%) in the spray solution. X-ray diffraction patterns showed that the films are polycrystalline in nature and the preferred growth direction of the undoped film shifts to (200) for Nb-doped films. Atomic force microscopy study shows that the surface morphology of these films vary when doping concentration varies. The negative sign of Hall coefficient confirmed the n-type conductivity. Resistivity of $\sim 4.3 \times 10^{-3}$ Ω cm, carrier concentration of $\sim 5 \times 10^{19}$ cm^{-3}, mobility of ~ 25 cm^2 V^{-1} s^{-1} and an average optical transmittance of $\sim 70\%$ in the visible region (500–800 nm) were obtained for the film doped with 0.5 at.% niobium.

Introduction

Transparent and conducting oxide (TCO) thin films have attracted a great deal of attention because of their unique nature of low resistivity and high transmittance in the visible range of solar spectrum [1–9]. These oxide thin films are extensively used for a variety of applications which include architectural windows, flat panel displays [2], thin film photovoltaics [3], smart windows [4] and polymer-based electronics [5]. SnO$_2$-based thin films have been widely studied because they are stable towards atmospheric conditions, chemically inert and mechanically hard and they can resist high temperatures [10]. These properties of SnO$_2$ have aroused great interest in the development of a short wavelength semiconducting laser, which has potential applications in manufacturing the next generation compact disc read heads [11]. In addition to their applications as optical windows for the solar spectrum, SnO$_2$ thin films have been employed successfully in touch sensitive switches, digital displays, electro chromic displays and gas sensors [12–14].

Pure and doped-SnO$_2$ thin films of various dopants have been prepared by various techniques, such as magnetron sputtering [15], sol–gel method [16], chemical vapour deposition (CVD) [17] and pulsed laser deposition [18]. Among these techniques, chemical spray pyrolysis method has a simple and inexpensive experimental arrangement and has the advantages like ease of adding dopands, reproducibility, high growth rate and mass production capability for uniform large area coatings, which are desirable for industrial and solar cell applications. Doping of various metals with TCO films has been demonstrated to be a simple and effective way to enhance the film characteristics and hence efforts have been made in this direction aiming at increasing the conductivity, transmission and stability of various TCOs [19, 20]. Doping is also often used to change the conductivity properties of oxide films. The niobium (Nb) atom has a similar outer shell electron configuration to tin, and has atomic number comparable to that of tin. Therefore, it is theorized that the Nb easily takes the place of the tin atoms in the tin oxide. To the best of the knowledge, no reports on the preparation of Nb-doped SnO$_2$ thin films by spray pyrolysis technique are available. Hence in this study, transparent and conductive Nb-doped tin oxide

V. Gokulakrishnan · S. Parthiban · K. Ramamurthi (✉)
Crystal Growth and Thin Films Laboratory, School of Physics,
Bharathidasan University, Tiruchirappalli 620 024, India
e-mail: krmurthin@yahoo.co.in

K. Jeganathan
Centre for Nanoscience and Nanotechnology, School of Physics,
Bharathidasan University, Tiruchirappalli 620 024, India

(SnO$_2$:Nb) thin films were prepared by chemical spray pyrolysis method with different doping levels of Nb and the effect of Nb on the structural, morphological, electrical and optical properties of tin oxide thin films was investigated as a function of various doping concentration in the spray solution (0–2 at.%).

Experimental details

Nb-doped SnO$_2$ thin films were deposited on glass substrates using an inbuilt spray pyrolysis experimental setup [21–23]. Stannous chloride (SnCl$_2$·2H$_2$O, Merck) and niobium chloride (NbCl$_2$, Sigma-Aldrich) were used as the sources of tin and niobium, respectively. Microscopic glass slides were used as substrates. The substrates were ultrasonically cleaned using distilled water, methanol and ethanol separately for 10 min, then the cleaned substrates were dried in hot oven. SnCl$_2$ (0.5 M) was dissolved in 5 ml of concentrated hydrochloric acid (HCl) and heated at 90 °C for 10 min and then diluted with methanol which formed the base solution for Nb doping. Then NbCl$_2$ was dissolved in double distilled water and added to the base solution to prepare the starting solution to deposit the Nb-doped SnO$_2$ films. The amount of NbCl$_2$ was varied to achieve different Nb/Sn atomic ratio percent (at.%) in the spray solution. Compressed air was used as the carrier gas. The airflow rate was maintained at 40 kg/cm^2. The distance between the spray nozzle and the substrate is about ~30 cm. The starting solution was sprayed on the substrates preheated to 400 °C. The spray time and interval was 3 s and 1 min, respectively. The total spray time was about 45 min and thickness of the films determined by using a filmetrics instrument was ~800 nm.

The structural characterization was carried out using Philips X'Pert Pro X-ray diffraction (XRD) system (Cu K$_\alpha$ radiation, $\lambda = 1.5405$ Å) in Bragg–Brentano geometry ($\theta/2\theta$ coupled) and surface morphology was studied by Atomic Force Microscope (AFM) (Agilent 5500). The optical transmittance (T%) was measured in the range of 300–1000 nm by double beam spectrophotometer (Ocean optics). Thickness of the film was determined by optical interference method using Filmertrics ($n = 1.9$, $\lambda = 500$ nm) and weight gain methods. The electrical studies were carried out using Hall effect measurement system (Ecopia HMS-3000) in van der Pauw configuration with a permanent magnet of 0.5 Tesla.

Results and discussion

Structural studies

The XRD patterns recorded for SnO$_2$ and Nb-doped SnO$_2$ thin films deposited at 400 °C are shown in Fig. 1. The
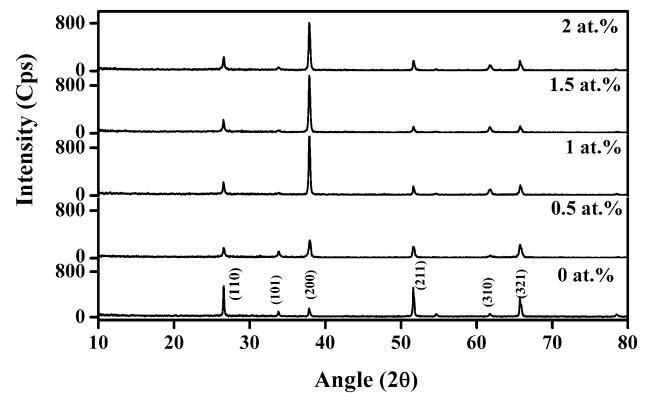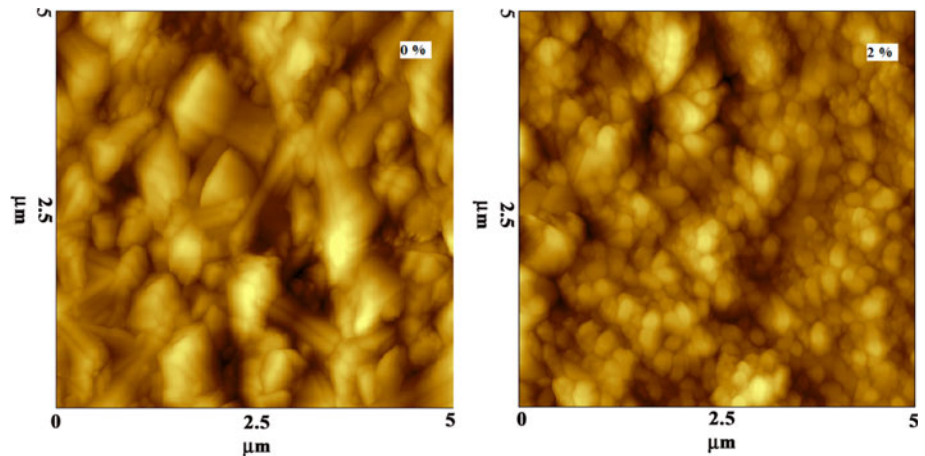

Fig. 1 XRD patterns of SnO$_2$ and SnO$_2$:Nb for various doping concentration

XRD studies reveal that the deposited films are polycrystalline. The lattice parameter values are calculated $a = b = 4.7468$ Å and $c = 3.1954$ Å by using XRD analysis software. The XRD peaks and the lattice parameters are in good agreement with the standard data (ICDD card no. 41-1445) of tetragonal structure. The observed intensities suggest a more random orientation of the crystallites in the films. The diffraction from the (110), (211) and (321) planes is relatively stronger in the pure SnO$_2$ films. In the case of 0.5 at.% Nb-doped SnO$_2$ film, XRD study reveals that the intensity of the diffraction peaks of SnO$_2$ film is reduced. However, the intensity of (200) peak emerges as the strongest for 1 at.% Nb doping. Further increase in Nb doping (1.5 and 2 at.%), does not produce appreciable changes in the intensity and growth orientation of the doped films. The change in the preferential orientation in SnO$_2$ films due to doping of various dopants was also well studied by many authors [23–25]. Agashe et al. [24] studied the effect of Sn incorporation on the growth mechanism of sprayed SnO$_2$ films and observed that the preferred growth direction changed from (110) to (200) direction as the Sn incorporation was increased. These results are also consistent with other studies where change of preferential orientation as a function of doping concentration was observed in SnO$_2$:In films [26]. Elangovan et al. [22, 23] observed that the fluorine and antimony doping in tin oxide thin films prepared by spray pyrolysis method changed the preferred direction from (211) to (200).

Morphology

The surface morphology of the transparent electrodes is another important factor in order to achieve high device performance in many applications such as photovoltaics and flat panel displays where the SnO$_2$ layer is used as an electrode. Figure 2 shows the AFM images of pure and 2 at.% Nb-doped SnO$_2$ films. Prior to the AFM measurements, the films were ultrasonically cleaned in ethanol and

Fig. 2 AFM images of Nb-doped SnO_2 thin films for 0 and 2 at.% Nb doping

blown dry with nitrogen gas. Root Mean Square (RMS) surface roughness of the Nb-doped SnO_2 films captured over an area of 5×5 μm is shown in Fig. 2. The RMS values of pure and Nb-doped SnO_2 films (2 at.%) are ~ 47 and ~ 89 nm, respectively. Thus, the SnO_2 film has a smooth surface when compare with that of the Nb-doped SnO_2 (2 at.%) film. The irregular shaped grains are less densely packed in the undoped films while for the 2 at.% Nb-doped films the grains are closely packed with appreciable changes in grain size. Thus, the surface morphology of the SnO_2 is modified by Nb doping. The reason for this morphological change is due to the change in the preferred growth orientation of the doped films.

Electrical properties

The electrical properties are estimated from room temperature Hall measurements in the van der Pauw configurations. The negative sign of Hall coefficient confirmed that the films are n-type semiconductors. The undoped SnO_2 film has a carrier concentration (*n*) of $\sim 6.1 \times 10^{19}$ (1.2×10^{19}) cm^{-3} and resistivity (*ρ*) of $\sim 4.7 \times 10^{-3}$ (4.63×10^{-3}) Ω cm. These values compare well with the corresponding values of sprayed SnO_2 films (given in parenthesis) reported by Elangovan et al. [27]. The resistivity of the film decreases with increasing Nb concentration up to 1.5 at.% and the resistivity increases for 2.0 at.% doping of Nb. On the other hand, Hall mobility of the Nb-doped films initially increases (0.5 at.% level), but then decreases gradually on increasing the doping level. The variation in electrical properties as a function of doping concentration is shown in Fig. 3. The electrical properties of doped SnO_2 thin films for various dopants obtained from various deposition techniques are summarized in Table 1. The mobility of the SnO_2:Nb is comparable with that of SnO_2:F and SnO_2:Al prepared by spray pyrolysis method and SnO_2:Ta and SnO_2:W films prepared by MOCVD and Pulsed plasma deposition (PPD) methods, respectively.
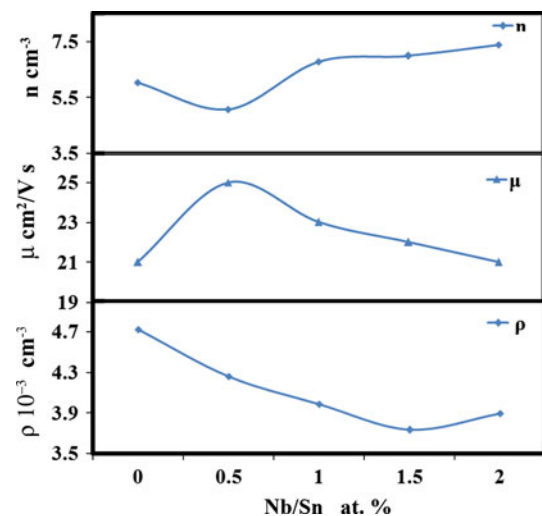

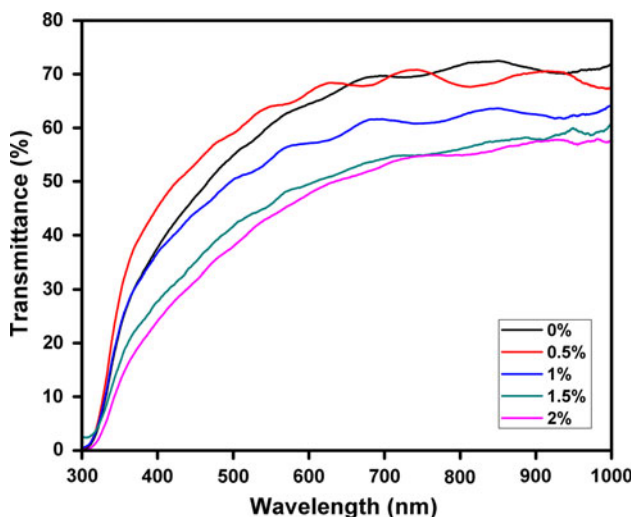**Fig. 3** Variation of electrical properties of SnO_2 as a function of Nb doping

A maximum mobility of ~ 25 cm^2 V^{-1} s^{-1}, carrier concentration of $\sim 5 \times 10^{19}$ cm^{-3} and a resistivity of $\sim 4.3 \times 10^{-3}$ Ω cm were achieved for 0.5 at.% Nb-doped SnO_2 films. Thus, in this study, 0.5% Nb doping seems to be the optimum level of doping in SnO_2 films which produced a combination of improved electrical property.

Optical properties

UV–Vis NIR spectra recorded for SnO_2 and Nb-doped SnO_2 films are represented in Fig. 4 which shows that the optical transmittance of Nb-doped SnO_2 films decreases with increasing Nb doping percentage. The decrease in transmittance at higher doping concentrations may be due to the increased scattering of photons by the crystal defects created by doping [32]. Nb-doped SnO_2 exhibits an average transmittance of $\sim 70\%$ (500–800 nm at 0.5 at.%) in the visible region. Further, the absorption edge shifts towards the longer wavelength region (red shift) as there is

Table 1 Comparison of electrical properties of SnO_2:Nb films with corresponding values of other works for various dopants

S no.	Dopants	μ (cm^2/V s)	ρ (Ω cm)	n (cm^{-3})	Techniques	References
1	SnO_2:Nb	25	4.25×10^{-3}	5.07×10^{19}	Spray	This study
2	SnO_2:Sb	12.03	2.86×10^{-4}	1.68×10^{21}	Spray	[23]
3	SnO_2:F	22.1	2.12×10^{-4}	13.30×10^{20}	Spray	[28]
4	SnO_2:Al	22.52	3.3×10^{-1}	8.41×10^{17}	Spray	[29]
5	SnO_2:Ta	24.5	2.01×10^{-4}	1.27×10^{21}	MOCVD	[30]
6	SnO_2:W	30	2.1×10^{-3}	9.6×10^{19}	PPD	[31]

Fig. 4 Optical transmittance spectra of pure and Nb-doped SnO_2 thin films

Fig. 5 $(\alpha h\upsilon)^2$ verses $(h\upsilon)$ plots for SnO_2 and SnO_2:Nb films with various concentrations
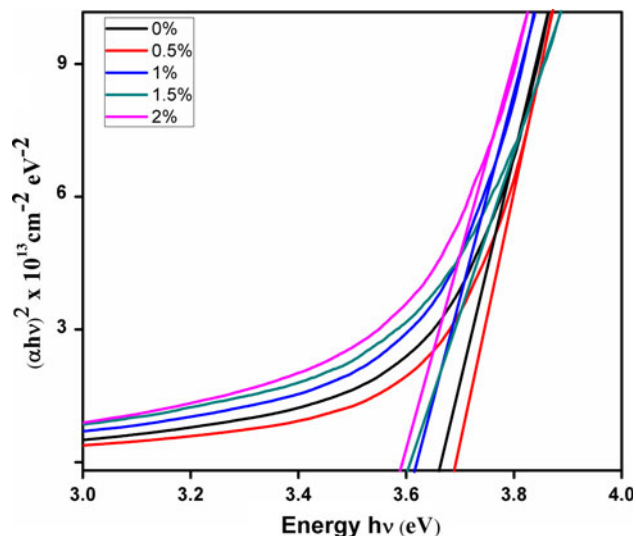
an increase of Nb concentration in the starting solution. From the transmission spectrum, if the multiple reflection of the thin film is neglected, the optical transmittance (T) is given by

$$\alpha = \frac{1}{t}\ln\left(\frac{1}{T}\right)$$

where α and t represent the optical absorption coefficient and the film thickness, respectively. The optical absorption coefficient was used to determine the indirect allowed energy band gap E_g of Nb-doped SnO_2 from the relation

$$(\alpha h\upsilon)^2 = A(h\upsilon - E_g)$$

where $h\upsilon$ is the photon energy, A is constant and h is the Planck's constant. The energy gap can be determined by the extrapolation of the linear region from the plot of $(\alpha h\upsilon)^2$ versus $h\upsilon$ near the onset of the absorption edge. The E_g value for pure single crystal SnO_2 has been reported to be in the range 3.57 eV which depends on the preparation method and deposition conditions [33–38]. In this experiment, for pure SnO_2 films, a band gap of $\sim$3.66 eV has been obtained, which is in good agreement with the

previously reported values of 3.62 eV [39] and 3.66 eV [40] for SnO_2. In the Fig. 5, it is observed that the energy band gap of the Nb-doped SnO_2 film slightly decreases with increasing Nb content in the solution.

Figure of merit

The quality of transparent conducting films can be determined by the figure of merit (φ), calculated from the optical transmittance and sheet resistance. It has been accomplished by Haacke [41]

$$\phi = \frac{T^{10}}{R_{sh}}$$

where T and R_{sh} are the transmittance and the sheet resistance, respectively. Thus, the higher value of the figure of merit represents for the better performance of the TCO films. Both the electrical conductivity and the transmittance of TCO should be as high as possible for application in solar cells [42]. Figure 6 shows the variation of the figure of merit with Nb concentration for the wavelength of 500 and 600 nm. In this investigation, the best value of the
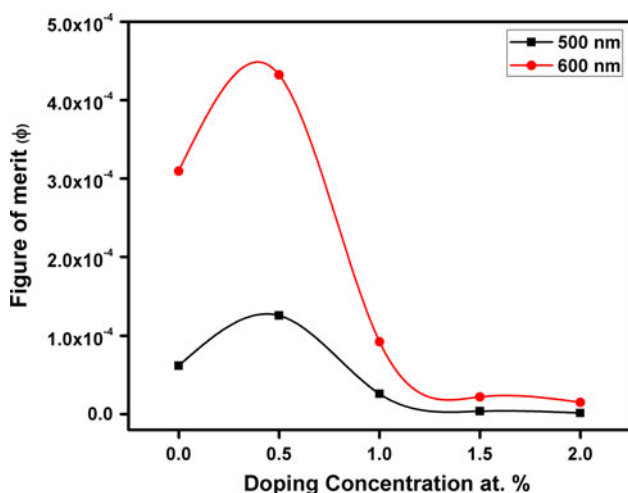
Fig. 6 The variation of the figure of merit of SnO_2 as a function of Nb doping concentrations

figure of merit (φ) was obtained for the films prepared with 0.5 at.% Nb doping and its value is $4.43 \times 10^{-4} \ \Omega^{-1}$ at 600 nm. Therefore, it can be concluded that the films deposited with such dopant level can perform better role as a window layer in solar cells.

Conclusions

Niobium-doped transparent conducting tin oxide thin films were deposited on glass substrates by chemical spray pyrolysis method at a substrate temperature of 400 °C. The XRD studies confirmed polycrystalline nature of SnO_2 and SnO_2:Nb films with tetragonal structure and the preferred orientation of SnO_2 is shifted to (200) peak for 1–2 at.% of Nb doping. This change in the growth orientation due to Nb doping is significantly influenced the surface morphology of these films. Hall measurements show that the 0.5 at.% doped film possesses the resistivity, carrier con centration and Hall mobility of $\sim 4.3 \times 10^{-3} \ \Omega$ cm, $\sim 25 \ cm^2 \ V^{-1} \ s^{-1}$ and $\sim 5 \times 10^{19} \ cm^{-3}$, respectively. The average optical transmittance of SnO_2:Nb (0.5 at.%) is $\sim 70\%$ in the range of 500–800 nm.

References

1. Minami T (2000) MRS Bull 25:38
2. Chacko S, Junaid Bushiri M, Vaidyan VK (2006) J Phys D 39:4540
3. Tala-Ighi R, Boumaou M, Belkaïd MS, Maallemi A, Melhaniand K, Iratni A (2006) Sol Energy Mater Sol Cells 90:1797
4. Purushothaman KK, Dhanashankar M, Muralidharan G (2009) Curr Appl Phys 9:67
5. Shrotriya V, Li G, Yao Y, Chu C-W, Yang Y (2006) Appl Phys Lett 88:073508
6. Yang Y, Jin S, Medvedava JE, Ireland JR, Metz AW, Ni J, Hersam MC, Freeman AJ, Marks TJ (2005) J Am Chem Soc 127:8796
7. Lin JM, Zhang YZ, Ye ZZ, Gu XQ, Pan XH, Yang YF, Lu JG, He HP, Zhao BH (2009) Appl Surf Sci 255:6460
8. Furubayashi Y, Hitosugi T, Yamamoto Y, Inaba K, Kinoda G, Hirose Y, Shimada T, Hasegawa T (2005) Appl Phys Lett 86:252101
9. He JH, Wu TH, Hsin CL, Li KM, Chen LJ, Chueh YL, Chou LJ, Wang ZL (2006) Small 2:116
10. Wongcharoen N, Gaewdang T (2007) In: Proceedings of ISES World Congress, vol 1269
11. Cao H, Qiu X, Liang Y, Zhang L, Zhao M, Zhu Q (2006) Chem Phys Chem 7:497
12. Martel A, Caballero-Briones F, Quintana P, Bartolo P (2007) Surf Coat Tech 201:4659
13. Wang S, Huang J, Zhao Y, Wang S, Wu S, Zhang S (2006) Mater Lett 60:1706
14. Feng X, Ma J, Yang F, Ji F, Zong F, Luan C, Ma H (2008) Mater Lett 62:1779
15. Wang Y, Ma J, Ji F, Yu X, Ma H (2005) J Lumin 114:71
16. Deng H, Kong J, Yang PX (2009) J Mater Sci Mater Electron 20:1078
17. Sundqvist J, Lu J, Ottosson M, Harsta A (2006) Thin Solid Films 514:63
18. Kim H, Auyeung RCY, Pique A (2008) Thin Solid Films 516:5052
19. Lewis BG, Paine DC (2000) MRS Bull 25:22
20. Minami T (2005) Semicond Sci Technol 20:S35
21. Elangovan E, Ramamurthi K (2003) J Opto Electron Adv Mater 5:45
22. Elangovan E, Shivashankar SA, Ramamurthi K (2005) J Cryst Growth 276:215
23. Elangovan E, Singh MP, Ramamurthi K (2004) Mater Sci Eng B 113:143
24. Agashe C, Takwale MG, Bhide VG, Mahamuni S, Kulkarni SK (1991) J Appl Phys 70:7382
25. Agashe C, Mahamuni S (1995) Semicond Sci Technol 10:172
26. Manoj PK, Joseph B, Vaidyan VK, Sumangala Devi Amma D (2007) Ceram Int 33:273
27. Elangovan E, Singh MP, Dharmaprakash MS, Ramamurthi K (2004) J Opto Electron Adv Mater 6:197
28. Elangovan E, Ramamurthi K (2005) Thin Solid Films 476:231
29. Bagheri-Mohagheghi M-M, Shokooh-Saremi M (2004) J Phys D 37:1248
30. Lee SW, Kim Y-W, Chen H (2001) Appl Phys Lett 78:350
31. Huang YW, Zhang Q, Li GF, Yang M (2008) Mater Charact 60:415
32. Van Vlack LH, Wesley A (1998) Elements of materials science and engineering. Thomson Press, Faridabad
33. Summit R, Marley JA, Berrelli NF (1964) J Phys Chem Solids 25:1465
34. Gu F, Wang SF, Lu MK, Cheng XF, Liu SW, Zhou GJ, Xu D, Yuan DR (2004) J Cryst Growth 262:182
35. De Souza AE, Monteiro SH, Santilli CV, Pulcinelli SH (1997) J Mater Sci Mater Electron 8:265
36. Leite ER, Bernardi B, Longo E, Varela JA, Paskocimas CA (2004) Thin Solid Films 449:67
37. Tsunekawa S, Fukuda T, Kasuya A (2000) J Appl Phys 87: 1318
38. Shanthi S, Subramanian C, Ramasamy P (1999) J Cryst Growth 197:858

39. Wang Y, Brezesinski T, Antonietti M, Smarsly B (2009) ACS Nano 3:1373
40. Korotkov RY, Gupta R, Ricou P, Smith R, Silverman G (2008) Thin Solid Films 516:4720
41. Haacke G (1976) J Appl Phys 47:4086
42. Chopra KL, Paulson PD, Dutta V (2004) Prog Photovolt Res Appl 12:69